Available online at www.sciencedirect.com
ScienceDirect
Earth and Planetary Science Letters 256 (2007) 12–27
EPSL
www.elsevier.com/locate/epsl

# Densities of metapelitic rocks at high to ultrahigh pressure conditions: What are the geodynamic consequences?

Hans-Joachim Massonne [a,*], Arne P. Willner [a,b], Taras Gerya [c]

[a] Institut für Mineralogie und Kristallchemie, Universität Stuttgart, Azenbergstr. 18, D-70174 Stuttgart, Germany
[b] Institut für Geologie, Mineralogie und Geophysik, Ruhr Universität, D-44780 Bochum, Germany
[c] Institut für Geophysik, Eidgenössische Technische Hochschule, HPP L 8.1, ETH-Hoenggerberg, CH-8093 Zürich, Switzerland

Received 16 February 2006; received in revised form 22 June 2006; accepted 7 January 2007
Available online 13 January 2007
Editor: G.D. Price

**Abstract**

Current geodynamic models of continental collision involving (ultra)high pressure complexes imply that even deeply subducted continental crust is significantly lighter than the ultrabasic upper mantle. To test this implication, we have investigated density changes of major components of continental crust, in particular metagreywacke and metapelite, as a function of pressure and temperature using a Gibbs free energy minimization approach. Pseudosections were calculated for fixed chemical compositions and the $P$–$T$ range of 10–40 kbar, 600–1000 °C. Selected compositions were those of natural psammopelitic rocks, average crustal components, various theoretical mixtures of quartz, plagioclase, illite, chlorite and Fe,Ti-oxides, and finally mid-ocean ridge basalt and lherzolite for comparison. Calculated densities were presented as density maps (isochors in $P$–$T$ diagrams).

In general, observed densities of psammopelitic rocks increase with rising pressure due to the formation of advancing amounts of garnet, Na-pyroxene, and kyanite. A common assemblage, for instance, at 25 kbar/800 °C consists of phengite, quartz, jadeite, garnet, kyanite, magnetite, and rutile. After overstepping the quartz–coesite transition the density of a mean psammopelitic rock (3.35 g/cm$^3$) is almost as high as that of garnet lherzolite. Calculations with other pelitic compositions demonstrate that the resulting densities (up to 3.5 g/cm$^3$) can even exceed that of a garnet lherzolite due to high contents of garnet.

Our calculations suggest that (i) even non-basic crustal material can sink into the Earth's mantle to fertilize it and (ii) the proportion of low-density granitic rocks in deeply subducted continental crust must be relatively high to claim buoyancy forces for a return of this crust to the surface.


*Keywords:* metapelites; density; ultrahigh pressures; pseudosections; subduction; crustal delamination

## 1. Introduction

Most of the recently published geodynamic scenarios on the collision of continental plates (e.g., [1–3]) imply that continental crust is subducted to depths of 100 km or more compatible with occurrences of coesite and microdiamonds in metamorphic rocks of the continental

* Corresponding author. Tel.: +49 711 68581222, +49 711 68581225; fax: +49 711 68581222.
*E-mail address:* h-j.massonne@mineralogie.uni-stuttgart.de (H.-J. Massonne).

0012-821X/$ - see front matter © 2007 Elsevier B.V. All rights reserved.
doi:10.1016/j.epsl.2007.01.013

crust (e.g., [4–6]). Furthermore, these scenarios imply the return of deeply subducted continental crust by buoyancy forces requiring that the continental crust is significantly less dense than the ultrabasic upper mantle at corresponding depths. However, this could be a prejudice based on the situation at shallower depths where many ordinary rocks such as orthogneisses, consisting mainly of quartz and feldspar, have, indeed, densities still below a value of 3.0 g/cm$^3$. However, simplified calculations for specific crustal units (e.g. lower crust) have already demonstrated [7,8] that the densities of such rocks can exceed this value when pressures had increased to 12 kbar and more ($T$>500 °C). This density increase is, among others, due to garnet- and Na-clinopyroxene-forming reactions as is best demonstrated by basic rock compositions transforming to eclogites which are significantly denser than the lherzolites of the Earth's upper mantle.

In spite of the above cited density calculations there is hardly anything known about precise density data as a function of rock composition and $P$–$T$ conditions. For that reason, we have intended to fill this gap using internally-consistent thermodynamic data sets of rock-forming minerals including their solid solution properties. These calculations were undertaken for the critical $P$–$T$ range >10 kbar, >600 °C which is suitable to discuss the density changes in deeply subducted rocks of continental affinity or at least in such rocks subjected to pressure increase, for instance, due to mere thickening of continental crust by collision of continental plates. Our main target was the group of clastic sediments but we also considered other rock types which altogether make up more than 90% of the continental crust.

## 2. Method of calculation and selected compositions

In order to calculate densities of rocks with fixed composition at any $P$–$T$ conditions, we used thermodynamic data of rock-forming minerals and a corresponding algorithm to find the equilibrium mineral assemblage and mineral compositions yielding the minimum Gibbs energy for given $P$, $T$, and rock composition. The resulting molar abundances ($x_1$, $x_2$,...,$x_n$) of coexisting minerals (number $n$) and the compositions of the (solid solution) phases and, thus, their molar masses ($m_1$, $m_2$,...,$m_n$) and molar volumes ($V_1$, $V_2$,...,$V_n$) allow to compute the density of the bulk rock as the ratio of the sum of molar masses multiplied with molar abundances ($x_1 \cdot m_1 + x_2 \cdot m_2 + x_n \cdot m_n$) to the sum of molar volumes multiplied with molar abundances ($x_1 \cdot V_1 + x_2 \cdot V_2 + x_n \cdot V_n$) of coexisting minerals. The minimum Gibbs energy relation for a specific rock composition was calculated for a net of $P$–$T$ conditions within a given $P$–$T$ frame to yield a so-called pseudosection.

We used the thermodynamic data set of Holland and Powell [9] for minerals and aqueous fluid. Virtually all rock-forming minerals (but no silicate melt) with significant solid solution behaviour, relevant for this study, can be sufficiently approached by these data although a number of simplifications are included such as a limited number of end members for a specific solid solution model (e.g., garnet is assumed to be composed of three end members only). The corresponding solid solution phases were (used activity model cited): 1) Ca-amphibole (Cam) composed of the end members tremolite, tschermakite, pargasite, glaucophane, ferroactinolite [10]; 2) biotite (Bt): phlogopite, annite, eastonite, ordered biotite [11]; 3) chlorite (Chl): clinochlore, amesite, daphnite, Al-ferrochlorite [12]; 4) chloritoid (Ctd): magnesiochloritoid, ferrochloritoid [9]; 5) epidote (Ep): clinozoisite, epidote, ferroepidote [13]; 6) garnet (Grt): almandine (alm), grossular (gross), pyrope (pyrop) [10]; 7) clinopyroxene (Cpx): jadeite (jad), diopside, hedenbergite [14,15]; 8) Na-amphibole (Nam): tremolite, tschermakite, glaucophane, ferroglaucophane [16]; 9) olivine (Ol): forsterite, fayalite [9]; 10) orthopyroxene (Opx): enstatite, ferrosilite, ordered orthopyroxene, Mg-Tschermak's molecule [9]; 11) paragonite (Pg): paragonite, margarite [16]; 12) plagioclase (Pl): anorthite, albite [16]; 13) potassic white mica (Kwm): muscovite, Mg–Al-celadonite (MAcel), $Fe^{2+}$–Al-celadonite (FAcel), paragonite (parag) [11]; 14) spinel (Spl): spinel, hercynite [9]; 15) talc (Tlc): talc, Fe-talc, Tschermak's talc [9]. All other solid phases (rutile, quartz, lawsonite, K-feldspar, magnetite and titanite) as well as $H_2O$ were treated as pure phases. Pseudosections calculated in the system $K_2O$–$Na_2O$–CaO–MgO–FeO–$Fe_2O_3$–$Al_2O_3$–$TiO_2$–$SiO_2$–$H_2O$ as in our case or subsystems of it with the above thermodynamic data have been repeatedly presented in the literature (e.g., [17–20]) yielding phase relations which are compatible with the common view of metamorphic petrologists.

The above simplifications of the mineral compositions, which include lacking Ti and $Fe^{3+}$ contents in phases such as amphibole, clinopyroxene, and mica, can result only in approximations of true densities of rocks in the deep Earth. This is also true in regard of the thermodynamic data used. For instance, we found the $P$–$T$ position of the reaction talc+phengite=biotite (actually phlogopite)+kyanite+quartz+$H_2O$ in the subsystem $K_2O$–MgO–$Al_2O_3$–$SiO_2$–$H_2O$ to lie at temperatures of more than 100 °C above the temperatures determined

experimentally by Massonne and Schreyer [21] (see also [22]). As biotite is thermodynamically less well known than phengite, kyanite, and talc, it is likely that the calculations with the thermodynamic data set of Holland and Powell [9] underestimate the stability field of biotite somewhat. There are further reasons why our density calculations can only be approximations: 1) A typical behaviour of metamorphic rocks is to equilibrate not perfectly during prograde metamorphism (thus, garnet cores and rims, typically, show different compositions) and hardly during retrogression. The thermodynamic calculations, however, imply perfect equilibration. 2) Water contents of a rock change with metamorphic conditions. At granulite facies conditions rocks can be almost dry. If such granulites, as typical rocks of the lower crust, would be subducted at moderate temperatures (600–700 °C) during continent–continent collision it would be likely that such rocks do not absorb significant amounts of water (compare with our calculations below) but remain dry as they are. This behaviour cannot be simulated with our calculations. Instead, we intended to consider a water-saturated rock by achieving calculations with rock compositions rich in $H_2O$. As a result of these calculations free $H_2O$ should be in excess but its amount is ignored for the calculated densities. 3) Our calculation method cannot either modify the given $Fe^{2+}$–$Fe^{3+}$ contents. We assumed about 10 to 16% of the total iron to be trivalent as magnetite or epidote are common phases in rocks addressed here. It could be that these estimated $Fe^{3+}$ contents are too high. For instance, if less $Fe^{3+}$ and, thus, less magnetite but more almandine (as carrier of $Fe^{2+}$) would occur a slight density increase compared to the calculated value must be considered according to the equation (at high $P$–$T$ conditions): 1 magnetite + 1 kyanite + 2 quartz (total molar volume 13.40 $cm^3$) = 1 almandine (11.51 $cm^3$/mol) + 0.5$O_2$. 4). MnO contents of rocks were ignored in our calculations. These contents would, for instance, enlarge the stability field of garnet (see, e.g., [23]) in our pseudosections. However, the amounts of early formed Mn-rich garnet are very small as the MnO contents in the here considered rocks are low (see Table 1). For this reason, the density change in regard to the calculated data without MnO is negligible.

For the calculations we applied the DEKAP code by Gerya et al. [17], which is based on a Gibbs free energy minimization approach, for the $P$–$T$ frame 10–40 kbar and 600–1000 °C suggesting that these conditions are the limits of relevant $P$–$T$ conditions for deeply subducted or deeply buried continental crust during continent–continent collision. In fact, thermodynamic data for simply composed melts such as those of feldspar components are present in the data set by Holland and Powell [9] but a reasonable thermodynamic mixing model for complex silicate melts in our nine oxide-component system is still lacking. For this reason, no silicate melt was considered in the above $P$–$T$ frame. Thus, the phase relations calculated for the high-temperature portion within this frame are metastable. This statement results from melting experiments with $H_2O$ bound only to silicate phases (e.g., [24,25]). According to experiments by Patiño Douce and McCarthy [26] silicate melt will appear in tonalitic rocks

Table 1
Rock compositions used for the calculation of pseudosections

| | Upper continental crust | Average sediment | Average pelagic clay | Mix 1 | Mix 2 | Mix 3 | Mix 4 | Fjortoft gneiss | Saidenbachite | N-MORB | Peridotite |
|---|---|---|---|---|---|---|---|---|---|---|---|
| $SiO_2$ in wt.% | 64.63 | 62.77 | 57.03 | 58.78 | 54.84 | 64.53 | 51.34 | 53.60 | 63.24 | 49.67 | 45.89 |
| $TiO_2$ | 0.49 | 0.73 | 0.82 | 1.13 | 1.16 | 1.08 | 1.08 | 1.50 | 0.73 | 1.29 | 0.09 |
| $Al_2O_3$ | 14.90 | 13.12 | 16.93 | 20.28 | 22.52 | 17.70 | 20.10 | 23.60 | 18.50 | 16.10 | 1.57 |
| FeO | 3.75 | 4.28 | 7.58 | 6.46 | 7.05 | 4.69 | 11.44 | 11.10 | 5.25 | 7.63 | 7.20 |
| $Fe_2O_3$ | 0.74 | 0.84 | 1.49 | 1.16 | 1.22 | 0.98 | 1.76 | 1.40 | 0.65 | 1.25 | 0.32 |
| CaO | 4.12 | 8.76 | 1.39 | 0.49 | 0.49 | 0.67 | 0.50 | 0.85 | 0.87 | 11.42 | 1.16 |
| MgO | 2.16 | 3.00 | 3.71 | 3.96 | 4.39 | 2.69 | 7.51 | 3.45 | 2.58 | 7.66 | 43.46 |
| MnO | 0.08 | 0.09 | 0.09 | 0.09 | 0.09 | 0.09 | 0.09 | 0.15 | 0.06 | 0.16 | 0.11 |
| $K_2O$ | 3.31 | 2.77 | 3.21 | 3.75 | 4.24 | 3.19 | 2.43 | 2.45 | 3.39 | 0.09 | 0.04 |
| $Na_2O$ | 3.82 | 1.65 | 5.75 | 1.85 | 1.93 | 2.34 | 1.65 | 0.40 | 2.65 | 2.74 | 0.16 |
| $H_2O$ | 2.00 | 2.00 | 2.00 | 2.05 | 2.06 | 2.03 | 2.10 | 1.50 | 2.08 | 2.00 | 0.00 |
| Sum | 100.00 | 100.00 | 100.00 | 100.00 | 100.00 | 100.00 | 100.00 | 100.00 | 100.00 | 100.00 | 100.00 |

For data sources see text. All analyses were normalized to 100 wt.% after adding about 2 wt.% of $H_2O$ (Fjortoft gneiss only 1.5 wt.%) to the rock to ensure $H_2O$ in excess for (at least a wide range of) the $P$–$T$ conditions of the pseudosection. For peridotite (the originally given $Cr_2O_3$ content was taken as $Fe_2O_3$, the NiO content of 0.29 wt.% was ignored but is included in the sum, the $K_2O$ content of 0.12 wt.% was reduced to 0.04 wt.%) no water was given but the DEKAP code for calculating pseudosections adds a minor quantity of water to any dry composition, if a minor amount of OH-minerals can be stable.

at about 865 °C at 10 kbar, 890 °C at 15 kbar, and at 900 °C at 33 kbar. For psammopelitic compositions the quoted temperatures are about 30 °C higher. An optimal resolution of 200 bar and 2 °C was used for stepwise calculation of the minimum Gibbs energy within the selected $P$–$T$ range. For each $P$–$T$ date a list is produced containing up to 10 coexisting phases (according to the Gibbs phase rule) with quantity, composition and density. In addition, maps using a specific colour code can be prepared using the listed data (for instance the concentration of a specific end member in a solid solution phase or the bulk rock density) and redrawn for presentation.

As psammopelitic rock compositions we used theoretical mixtures from quartz (pure $SiO_2$), plagioclase (oligoclase with An ~ 15 as an approximate mean plagioclase): 67.5 wt.% $SiO_2$, 18.5 wt.% $Al_2O_3$, 0.5 wt.% $Fe_2O_3$, 3 wt.% CaO, 0.5 wt.% $K_2O$, 10 wt.% $Na_2O$), illite (47.5 wt.% $SiO_2$, 0.5 wt.% $TiO_2$, 33.5 wt.% $Al_2O_3$, 2 wt.% FeO, 1.5 wt.% MgO, 9 wt.% $K_2O$, 1.5 wt.% $Na_2O$, 4.5 wt.% $H_2O$), chlorite (26 wt.% $SiO_2$, 20 wt.% $Al_2O_3$, 5 wt.% $Fe_2O_3$, 20 wt.% FeO, 16 wt.% MgO, 13 wt.% $H_2O$), and Fe,Ti-oxides (30 wt.% $TiO_2$, 5 wt.% $Al_2O_3$, 40 wt.% $Fe_2O_3$, 16 wt.% FeO, 2 wt.% MgO, 3 wt.% MnO, 4 wt.% CaO). Mix 1 had a weight proportion of these minerals of 25:12:40:20:3. For Mix 2, 3 and 4 we selected proportions of 18:12:45:22:3, 32:18:34:13:3, and 18:12:25:42:3, respectively. In spite of the above given $Fe_2O_3$, FeO and $H_2O$ contents in the minerals, trivalent iron in the four theoretical rock compositions Mix 1 to 4 is only half of that resulting from the above mineral compositions (due to reducing conditions at depth) and the water content of the bulk rock was set to somewhat more than 2 wt.% to ensure $H_2O$ excess conditions (see above).

In addition to the theoretical compositions, two natural psammopelitic rocks were used, which had experienced ultrahigh pressure conditions due to the detection of microdiamonds in these rocks: (1) a gneiss from the island of Fjortoft in the Norwegian Caledonides where Dobrzhinetskaya et al. [27] had reported microdiamonds, (2) a diamondiferous quartzo-feldspathic rock from the Saxonian Erzgebirge (called saidenbachite, see [28]). Both rocks had been analysed by conventional XRF techniques. Trivalent iron in Fjortoft gneiss and saidenbachite was chosen to be 10% of the total iron. Contents of $H_2O$ were selected to be similar to those of the theoretical compositions Mix 1 to 4.

The average compositions for sediment, pelagic clay, and upper continental crust are from McLennan [29]. Trivalent iron in these compositions was set to 15% of the total iron as discussed above. $H_2O$ contents were chosen to be 2 wt.% similar to the previous compositions. For comparison, an average garnet lherzolite [30] and a normal mid-ocean-ridge basalt (N-MORB) from the northern Mid-Atlantic Ridge [31], to which 2 wt.% of $H_2O$ (Table 1) were added, were considered. All these compositions, except for the peridotite, were plotted into an AKF diagram (Fig. 1) to visually relate these compositions to each other.

## 3. Results

The results of our calculations were presented in $P$–$T$ diagrams of Figs. 2–8. Representative calculated modal compositions for specific $P$–$T$ conditions (15 kbar–700 °C, 25 kbar–800 °C, 35 kbar–900 °C) are given in Tables 2–4. Fig. 2 shows a completely worked out pseudosection of composition Mix 4 as an example. Other pseudosections (Figs. 3–6) were simplified as follows: Small $P$–$T$ fields containing phases X and Y in addition to other (max. 8) phases between large fields with X or Y (+additional phases) were suppressed. Instead of these small fields an average line was drawn marking the appearance (= "in" or disappearance = "out") of X or Y. In case of the corresponding, often wider $P$–$T$ field for X = plagioclase and Y = jadeite, a thicker line was drawn (Figs. 2–6).

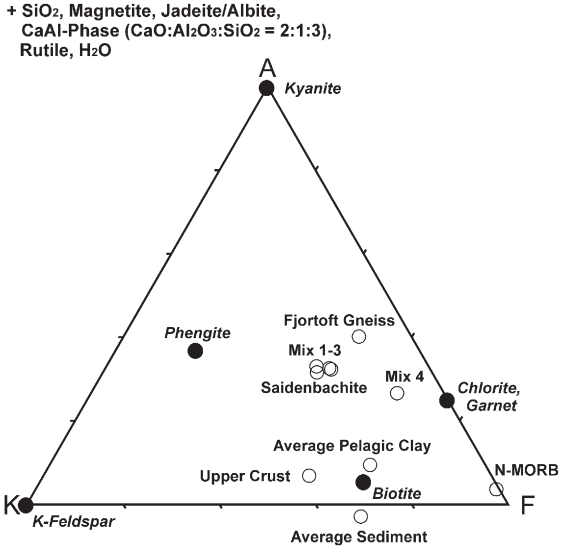


Fig. 1. Ten compositions (open circles) of Table 1 (without peridotite) plotted in a modified AKF diagram after projection from quartz/coesite, magnetite, rutile, $H_2O$ and an Na:Al = 1:1 phase (albite or jadeite as components of feldspar or clinopyroxene) as well as a Ca:Al = 1:1 phase (such as anorthite but grossular and clinozoisite are close to this proportion). Some common mineral compositions (closed circles) in psammopelitic rocks are shown for orientation.

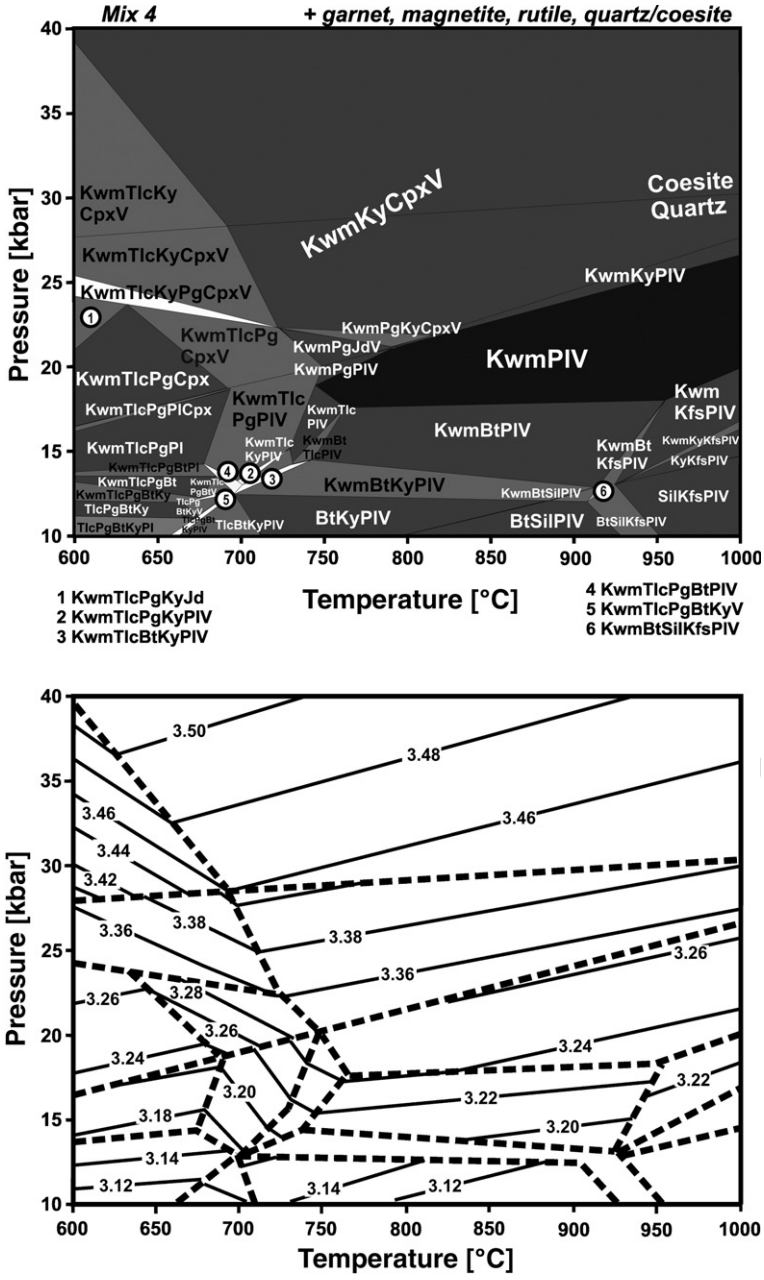


Fig. 2. Calculated pseudosection (at the top) and density chart (at the bottom, isochores in g/cm$^3$) for Mix 4. Abbreviations: Bt = biotite, Cpx = clinopyroxene, Kfs = K-feldspar, Kwm = potassic white mica, Ky = kyanite, Pg = paragonite, Pl = plagioclase, Sil = sillimanite, Tlc = talc, V = vapour ($H_2O$). Shading: white = divariant, light grey = trivariant, dark grey = quadrivariant, black = quintvariant assemblages.

Although selected $H_2O$ contents were not always sufficient to result in $H_2O$ excess conditions (relevant only for the low temperature, low pressure range of the selected *P–T* frame) the following general principles are valid:

1) For a wide high pressure (>20–25 kbar), high temperature (>750–800 °C) range a specific mineral assemblage is stable (e.g. kyanite–phengite(Kwm)–garnet–jadeite–quartz/coesite+magnetite, rutile, $H_2O$ for all psammopelitic compositions poor in Ca). As mineral compositions hardly change composition within this *P–T* range (see garnet in Figs. 4 and 6) there is also no significant change in modal composition (except quartz transformed to coesite; compare results shown for 25 kbar, 800 °C in Table 3 and for 35 kbar, 900 °C in Table 4; however, some

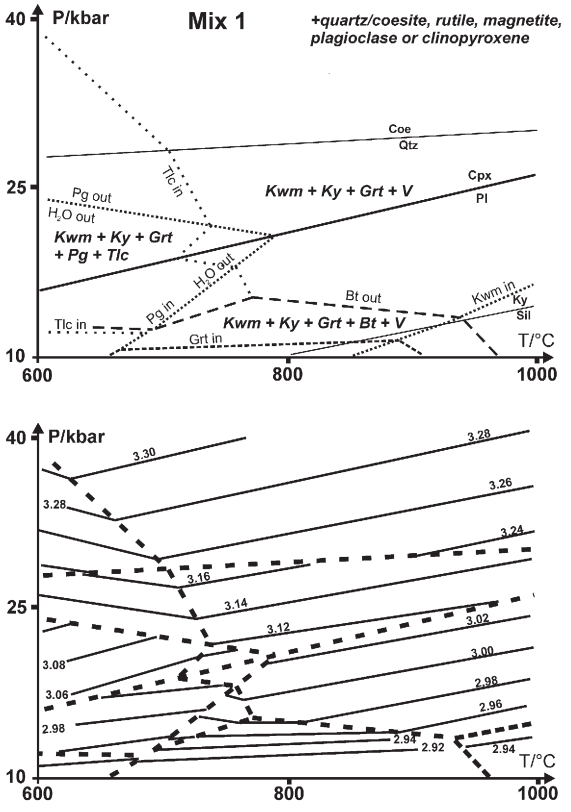


Fig. 3. Calculated pseudosection (at the top, simplified) and density chart (at the bottom, isochores in g/cm$^3$) for Mix 1. The appearance of lawsonite at pressures close to 40 kbar and temperatures somewhat above 600 °C is not shown here. Abbreviations: Grt = garnet and as in Fig. 2.

garnet increases towards higher pressures in the average sediment). Thus, the density change of the bulk rock (except the change related to the quartz–coesite transition) is predominantly due to the compressibility and expansivity of the minerals in this high pressure, high temperature assemblage. Thus, a decrease of density with rising temperature in the order of 0.0001 g·cm$^{-3}$·K$^{-1}$ or increasing pressure around 0.035 g·cm$^{-3}$ GPa$^{-1}$ can be deduced for all studied compositions.

2) In contrast to the above high pressure, high temperature range, many mineral reactions occur in the low temperature, lower pressure range of our selected *P–T* frame. These are generally related to dehydration reactions (see, breakdown of talc or paragonite in Figs. 2–5) which can lead to *P–T* fields where a density increase occurs with rising temperatures. The effect of these reactions on the density of the bulk rock is often minor. However, the reactions limiting paragonite towards high pressures (= "paragonite-out" close to 25 kbar) for pelitic compositions (Mixes 1–4, Fjortoft gneiss) can also result in a significant density change (0.05 g/cm$^3$ at 600 °C for Mix 3).

3) Significant density changes with increasing pressure can mainly be observed by three important reactions (except for the peridotite composition) which are: a) quartz–coesite transition (between 27 to 30 kbar), b) "biotite-out" (for most investigated compositions around 15 kbar) and "garnet-in", and c) formation of Na-rich clinopyroxene at the expense of plagioclase (omphacite can already be present at 10 kbar, jadeite close to 16 and 25 kbar at 600 °C and 1000 °C, respectively, for Ca-poor compositions such as saidenbachite, see clinopyroxene compositions in Tables 2–4).

These density changes can be relatively abrupt when caused by the quartz–coesite transition or the jadeite formation for compositions Mix 1 to 4, Fjortoft gneiss, saidenbachite, and average pelagic clay (all are relatively Ca-poor bulk rock compositions). However, such significant changes can also extend over a relatively wide

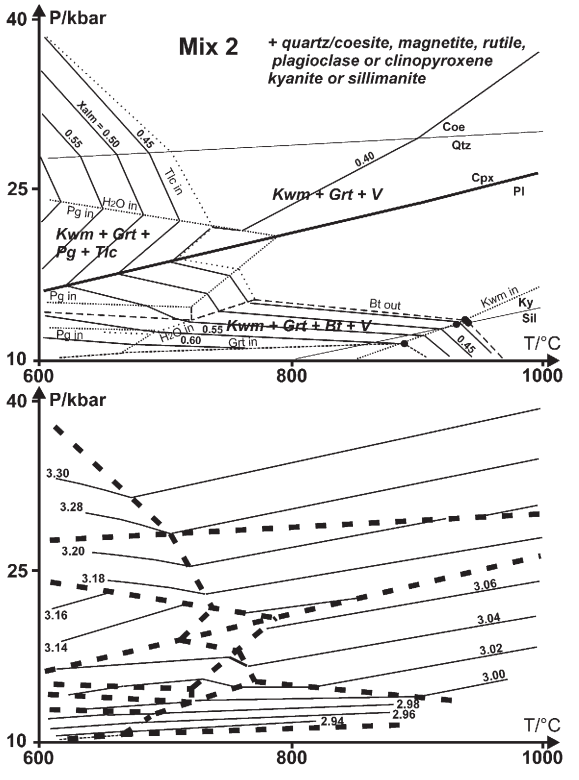


Fig. 4. Calculated pseudosection (at the top, simplified) and density chart (at the bottom, isochores in g/cm$^3$) for Mix 2. The pseudosections also show the variable garnet composition in terms of the molar fraction of almandine (Xalm). For lawsonite and abbreviations see Fig. 3.

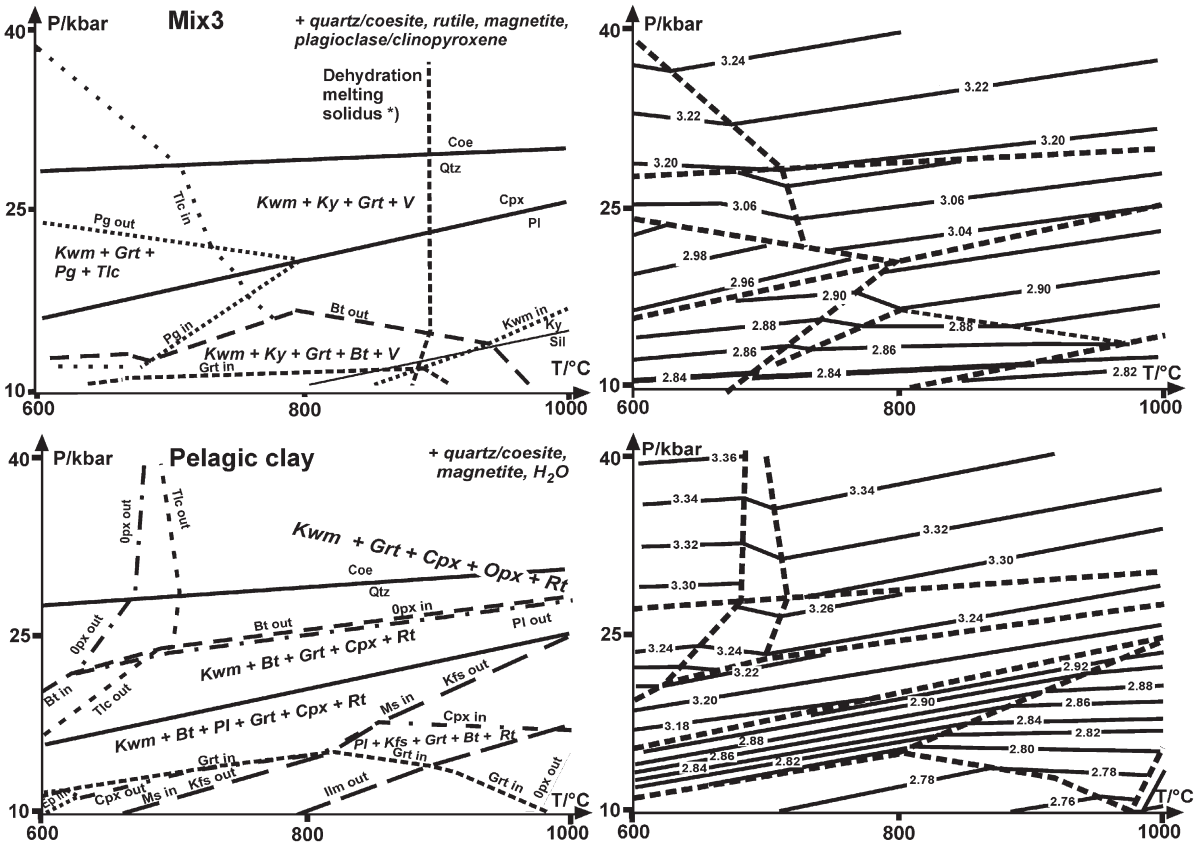


Fig. 5. Calculated pseudosections (left hand side, simplified) and density chart (right hand side, isochores in g/cm$^3$) for Mix 3 (at the top) and average pelagic clay (at the bottom). Abbreviations: Opx = orthopyroxene, Rt = rutile, and as in Fig. 2. *)The stippled curve in the left hand diagram for Mix 3 shows the melting curve by Patiño Douce and McCarthy [26] for a metagreywacke.

pressure range (see 10–20 kbar range also in Fig. 9) due to the wide solid solution ranges of garnet and omphacite. Such kind of change is most obvious for the N-MORB composition (according to Fig. 9b: 3.00 g/cm$^3$ at 10 kbar, 3.43 g/cm$^3$ at 18.5 kbar) but also large for other compositions (e.g. average upper continental crust).

Especially because of 3) the various studied rock compositions show different characteristics in the change of their bulk rock density relative to that for the peridotite which shows a more or less continuous density increase towards high pressures. As outlined above, the density increase of the N-MORB composition from 10 to 20 kbar amounts to about 0.45 g/cm$^3$ (~15%, according to Fig. 9b) resulting in overstepping the density of peridotite close to 18 kbar, when large amounts of omphacite are formed in the corresponding pressure range. Mix 4 and Fjortoft gneiss show the same signature, however, at a somewhat higher pressure (~21 kbar). After overstepping the quartz–coesite transition at ~30 kbar all these three compositions (N-MORB, Mix 4, Fjortoft gneiss) reach a density which is significantly higher than that of peridotite. The metapelitic composition Mix 4 is relatively rich in chlorite before medium grade metamorphism and garnet-rich at high *P–T* conditions, which might be related to the Fjortoft gneiss as well, and, thus, plots close to the A–F side of the compositional triangle of Fig. 1. As such relatively K-poor compositions are not rare among pelitic rocks, it is clearly demonstrated here that metapsammopelites can be denser than the Earth's upper mantle (= peridotite) after exceeding 20 (or 30) kbar (and corresponding temperatures). This is certainly due to a considerable enrichment of garnet in these rocks (Tables 3 and 4). The calculated high content of garnet (~30 wt.%) matches well with modal compositions of the Fjortoft gneiss.

The investigated K-rich (= phengite-rich at elevated pressure, = K-feldspar-rich at high grade metamorphism) metapsammopelites at least approach the density of peridotite after overstepping the quartz–coesite transition (Fig. 9). The same is true concerning the three investigated average compositions although they do not

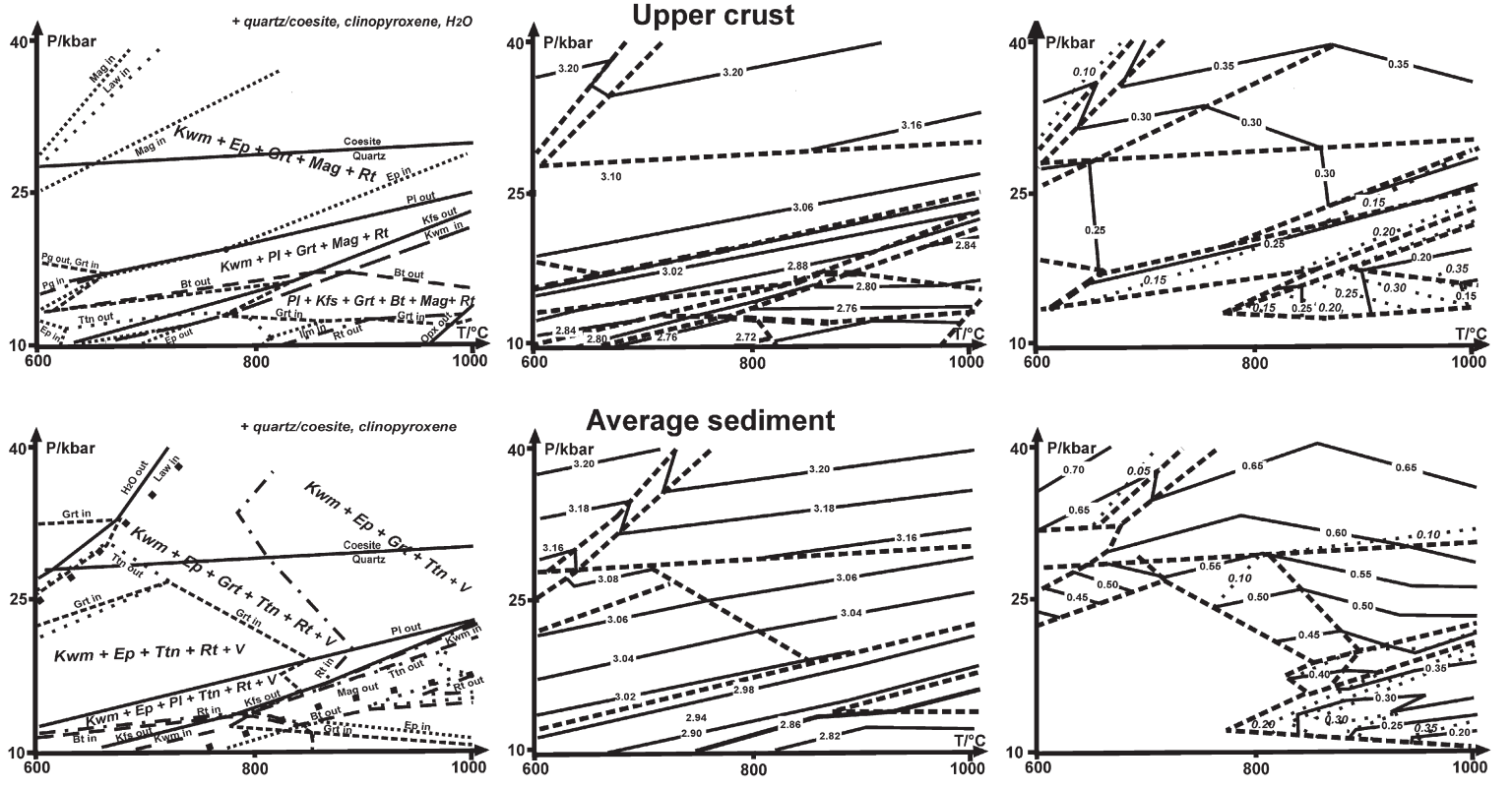


Fig. 6. Calculated pseudosections (left hand side, simplified), density charts (in the middle, isochores in g/cm$^3$), and variable composition of garnet (right hand side) for average upper continental crust (at the top) and average sediment (at the bottom). Xpyrope is shown by dotted lines in the right hand diagrams, Xgrossular by unbroken lines. Abbreviations: Ep = epidote, Ilm = ilmenite, Law = lawsonite, Mag = magnetite, Opx = orthopyroxene, Rt = rutile, Ttn = titanite, and as in Fig. 2.

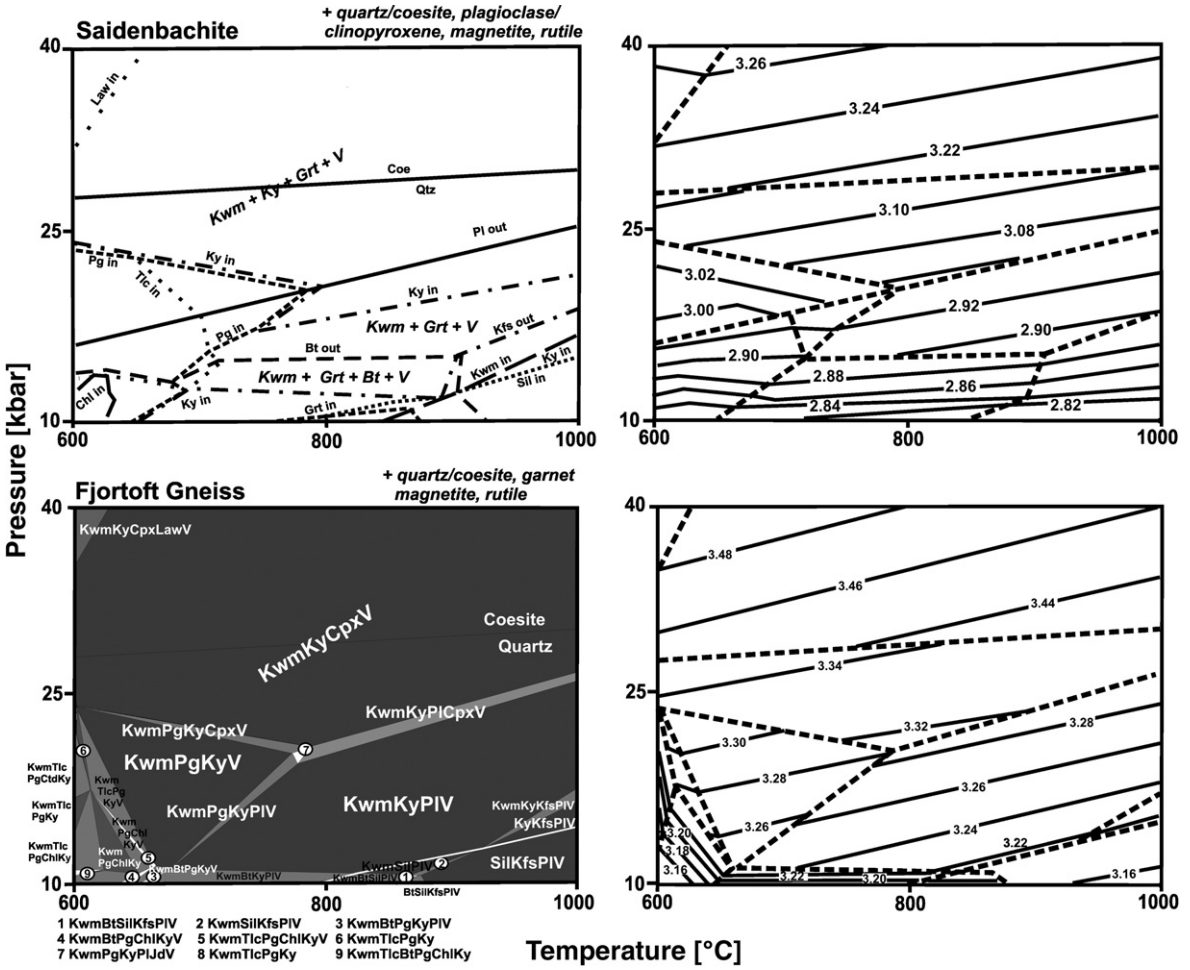


Fig. 7. Calculated pseudosections (left hand side) and density chart (right hand side, isochores in g/cm$^3$) for saidenbachite (at the top) and Fjortoft gneiss (at the bottom). Abbreviations: Chl = chlorite, Ctd = chloritoid, Law = lawsonite, and as in Fig. 2. Shading as in Fig. 2.

necessarily reflect existing rocks (they represent a compositional average of rocks behaving differently in terms of density). At the highest *P–T* conditions of Fig. 9 (40 kbar, 880 °C; 35 kbar, 1000 °C) the difference of average upper continental crust (lowest density of the investigated compositions) and peridote is still in the range of 0.15 g/cm$^3$ (~5%). For this particular average composition we observe a clear density increase between 12 and 20 kbar (related to Fig. 9b) from 2.74 to 3.03 g/cm$^3$ due to formation of increasing amounts of garnet and omphacite. However, this density increase is not sufficient to overstep the density of peridotite.

### *3.1. Possible consequences of the calculated rock densities*

With our new results geodynamic processes can be better elucidated or even correspondingly modified. All these processes discussed below are related either to sinking of material of the continental crust into the upper mantle or to buoyant ascent of this material from mantle depths in the order of several cm/year. Such speeds require appropriate density contrasts and viscosities of the rocks (see [32–34]) participating in the discussed geodynamic processes. In these processes most likely strong density fractionation is involved. It must be born in mind that melting processes might occur along a burial path towards high temperatures that cause, for instance, additional density contrasts between psammitic and pelitic compositions. In the presence of excess water larger amounts of melts can be produced in psammopelitic compared to metapelitic rocks as the psammopelites are compositionally closer to eutectic silicate melts. Thus, at $H_2O$ excess conditions melting further increases the density difference between a (anatectic) metapsammite and a metapelite. However,

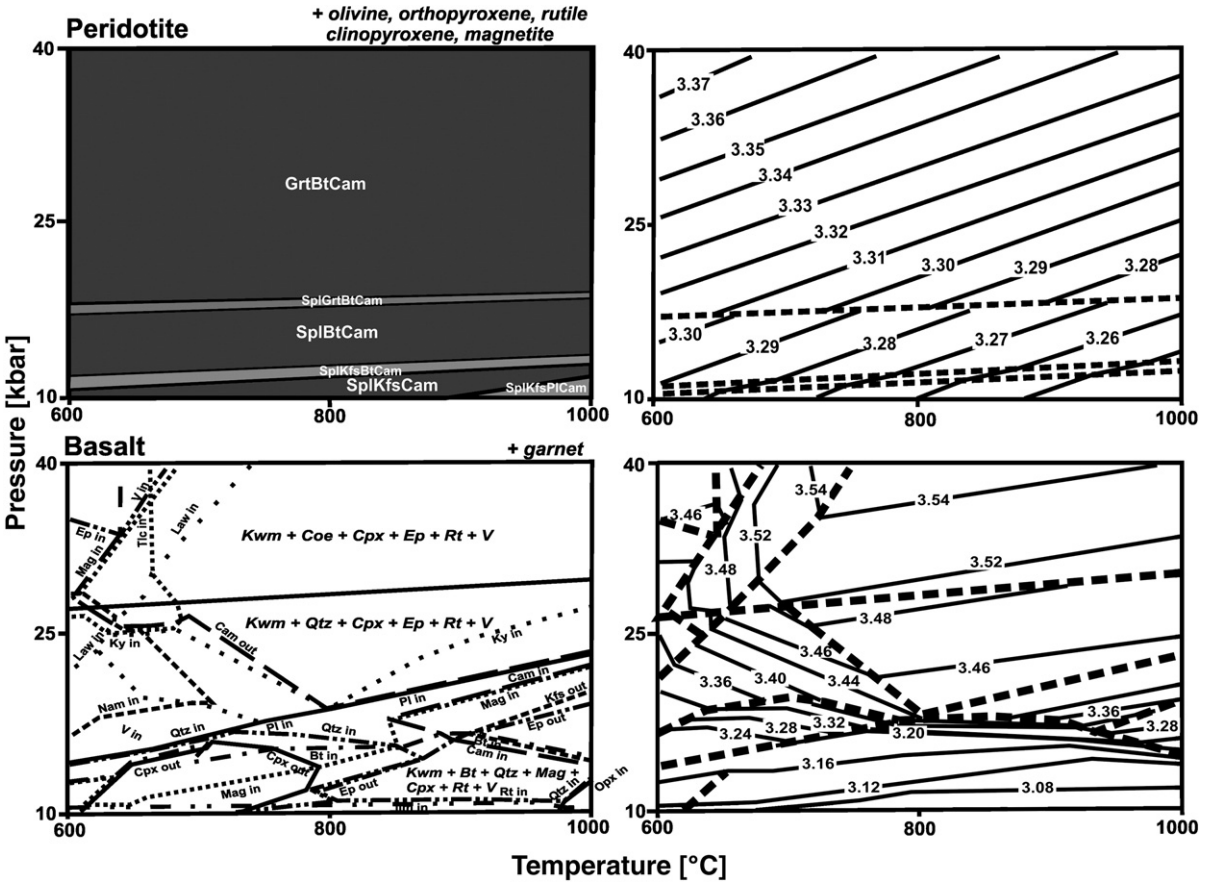


Fig. 8. Calculated pseudosections (left hand side) and density chart (right hand side, isochores in g/cm$^3$) for peridotite (at the top) and N-MORB (at the bottom). Abbreviations: Spl = spinel, Cam = Ca-amphibole and as in Fig. 2. Shading as in Fig. 2.

without free water larger amounts of melts would be produced in pelitic rocks because more $H_2O$ is bound to silicates (= micas) than in metapsammopelites.

### 3.1.1. Subduction of continental crust

To explain the origin of Phanerozoic orogenic belts with occurrences of ultrahigh pressure crustal material, various geodynamic scenarios have been developed which frequently suggest the subduction of one continental plate during continent–continent collision. A currently favoured model, for instance for the collision of the Sino–Korean craton with the Yangtze craton in Triassic times (~230 Ma ago) leading to the orogenic belt of the Dabie Shan and Sulu terrain in China [35], is the slab break-off model by Davies and von Blanckenburg [36]. This model, which is applied to other orogens as well (e.g., [37]), implies (1) the dragging of a continental crust down into the mantle by an adherent oceanic plate and (2) the buoyant ascent of the subducted continental plate after break-off of the oceanic slab which continues sinking. During the deep subduction of the continental plate coesite formed as, for instance, frequently indicated at least as preserved inclusion in zircon of the ultrahigh pressure gneisses of the Dabie–Sulu terrain (e.g., [38,39]). We conclude from the above calculations that the density of the deeply subducted (coesite-bearing) continental plate should have been close to that of the mantle. An assumed average continental crust consisting of 30% basic material (density at 800 °C, 30 kbar: 3.515 g/cm$^3$ according to our N-MORB), 30% of metasediments (density at 800 °C, 30 kbar: between 3.175 g/cm$^3$ (average sediment composition) and 3.441 g/cm$^3$ (Fjortoft gneiss): assumed mean: 3.25 g/cm$^3$), and 40% of granodioritic (see Table 1) upper continental crust (density at 800 °C, 30 kbar: 3.168 g/cm$^3$) has a density of 3.297 g/cm$^3$ which is very similar to that of peridotite (at 800 °C, 30 kbar: 3.328 g/cm$^3$). Therefore, in solid state such crustal material is virtually neutrally buoyant compared to the mantle. Significant negative buoyancy forces can only be created by increasing the proportion of denser rocks. Alternatively, positive

Table 2
Modal composition, bulk rock density (g/cm$^3$), and end member compositions of garnet, clinopyroxene, and phengite at 15 kbar and 700 °C resulting from the calculation with the DEKAP code applied to the rock compositions of Table 1

| | Average pelagic clay | Average sediment | Upper continental crust | Mix 1 (no $H_2O$) | Mix 2 (no $H_2O$) | Mix 3 | Mix 4 | Fjortoft gneiss | Saiden-bachite | MORB | Upper mantle |
|---|---|---|---|---|---|---|---|---|---|---|---|
| Quartz | 8.17 | 31.75 | 22.94 | 24.70 | 15.53 | 33.18 | 12.39 | 28.21 | 28.10 | | |
| Rutile | 0.56 | 0.24 | 0.34 | 0.80 | 0.83 | 0.74 | 0.83 | 1.17 | 0.51 | 0.99 | 0.07 |
| Clinopyroxene | 1.77 | 28.90 | 18.96 | | | | | | | | 5.48 |
| K white mica | 6.35 | 26.10 | 29.97 | 36.66 | 41.92 | 30.21 | 26.24 | 26.24 | 32.81 | 0.98 | |
| Biotite | 22.91 | | | | | | | | | | 0.39 |
| Garnet | 3.38 | | 0.45 | 12.11 | 13.49 | 6.95 | 31.06 | 29.29 | 12.85 | 17.34 | |
| Magnetite | 1.21 | | 0.61 | 1.96 | 2.09 | 1.60 | 1.61 | 1.31 | 0.54 | | 0.30 |
| Epidote | | 11.80 | | | | | | | | 14.50 | |
| Titanite | | 0.85 | | | | | | | | | |
| Kyanite | | | | 1.46 | 3.54 | | | 10.36 | | | |
| Plagioclase | 55.65 | 0.35 | 26.74 | 12.18 | 16.58 | 14.38 | 10.03 | | 23.96 | 22.73 | |
| Paragonite | | | | 5.05 | 0.34 | 8.88 | 6.30 | 3.42 | 0.51 | | |
| Talc | | | | 5.07 | 5.67 | 4.07 | 11.53 | | 0.72 | | |
| Ca-amphibole | | | | | | | | | | 43.46 | 0.18 |
| Orthopyroxene | | | | | | | | | | | 29.35 |
| Olivine | | | | | | | | | | | 63.25 |
| Spinel | | | | | | | | | | | 0.98 |
| **Density** | **2.8485** | **3.0125** | **2.8818** | **2.9739** | **3.0165** | **2.8770** | **3.1982** | **3.2606** | **2.9042** | **3.1765** | **3.2872** |
| Xalm | 0.6505 | | 0.6165 | 0.4853 | 0.4887 | 0.5022 | 0.5566 | 0.6474 | 0.5182 | 0.4851 | |
| Xpyrope | 0.1420 | | 0.1689 | 0.4583 | 0.4613 | 0.3944 | 0.4122 | 0.3382 | 0.3997 | 0.2342 | |
| Xgrossular | 0.2075 | | 0.2146 | 0.0564 | 0.0499 | 0.1034 | 0.0312 | 0.0647 | 0.0822 | 0.2807 | |
| Xjad | 0.3423 | 0.3437 | 0.3466 | | | | | | | | 0.1595 |
| XMAcel | 0.1539 | 0.1578 | 0.1653 | 0.1637 | 0.1635 | 0.1683 | 0.1662 | 0.1281 | 0.1677 | 0.1330 | |
| XFAcel | 0.3264 | 0.2000 | 0.2785 | 0.1036 | 0.1046 | 0.1193 | 0.1373 | 0.1308 | 0.1244 | 0.1186 | |
| Xparag | 0.0439 | 0.0365 | 0.0476 | 0.0959 | 0.0965 | 0.1008 | 0.1116 | 0.0927 | 0.1037 | 0.0837 | |

buoyancy can be promoted by partial melting of the crustal material under (ultra)high pressure and high temperature conditions (e.g., [32,33]). On the basis of the above consideration of densities alone, the slab break-off model cannot be ruled out to account for the Triassic ultrahigh pressure rocks in China. For instance, the portion of the subducted continental crust, which has not yet reached such great depths to transform quartz to coesite, can enhance the buoyancy forces. In addition, it is assumed by several authors of corresponding geodynamic models (e.g., [40]) that the transformation of quartz to coesite is widely impeded even in deeply subducted continental crust due to the fact that many of the corresponding rocks are virtually dry and/or hardly deformed. Nevertheless, the question arises if the entire subducted continental crust after the break-off of the oceanic slab will return to the Earth's surface. It might be that basic portions of the continental crust (commonly concentrated in the lower continental crust which *per definitionem* shows a higher velocity of seismic waves and is, thus, denser than the upper continental crust), can be separated from it to sink into the mantle. This could also concern metapelites when these rocks are so dense as, for instance, the Fjortoft gneiss. Indeed, in the ultrahigh pressure unit of the Dabie–Sulu terrain garnet-poor orthogneisses clearly dominate [41]. This could be an indication for the envisaged separation of denser and lighter continental crust during the subduction process which was hypothesized by Leech [8] and which is also the result of recent numerical experiments [34]. This density fractionation (gravitational ordering) process could even be of general importance for any continent–continent collisional event. By this process, low-density upper crustal material would be enriched in the continental crust, because denser intermediate to basic material will be depleted. Vice versa, the mantle beneath such a collisional belt could be fertilized for subsequent melting processes.

### *3.1.2. Delamination of the lithosphere with continental crust involved*

The subduction of continental crust is only one possibility although it appears to explain the existence of ultrahigh pressure rocks of crustal affinity satisfactorily. Continent–continent collision could also result in extended areas of continental crust thickened to approximately double normal thickness of continental crust. In regard of the collision of India and Asia this

Table 3
Modal composition, bulk rock density (g/cm$^3$), and end member compositions of garnet, clinopyroxene, and phengite at 25 kbar and 800 °C resulting from the calculation with the DEKAP code applied to the rock compositions of Table 1

| | Average pelagic clay | Average sediment | Upper crust | Mix 1 | Mix 2 | Mix 3 | Mix 4 | Fjortoft gneiss | Saiden-bachite | MORB | Upper mantle |
|---|---|---|---|---|---|---|---|---|---|---|---|
| Quartz | 15.91 | 31.81 | 30.12 | 29.09 | 20.61 | 38.57 | 18.52 | 27.84 | 34.28 | 9.38 | |
| Rutile | 0.63 | 0.20 | 0.36 | 0.85 | 0.88 | 0.79 | 0.88 | 1.20 | 0.54 | 1.09 | 0.07 |
| Clinopyroxene | 41.16 | 28.17 | 35.85 | 11.66 | 12.29 | 15.25 | 11.09 | 2.43 | 17.33 | 41.50 | 4.83 |
| K white mica | 22.21 | 25.34 | 30.35 | 35.97 | 41.07 | 29.71 | 25.30 | 24.86 | 31.93 | 1.00 | |
| Biotite | 9.51 | | | | | | | | | | 0.39 |
| Garnet | 9.21 | 1.09 | 1.60 | 15.33 | 17.19 | 8.98 | 41.65 | 29.03 | 12.45 | 37.52 | 3.60 |
| Magnetite | 1.37 | | 0.45 | 2.08 | 2.21 | 1.71 | 1.71 | 1.34 | 0.58 | | 0.30 |
| Epidote | | 12.40 | 1.28 | | | | | | | 9.51 | |
| Titanite | | 0.99 | | | | | | | | | |
| Kyanite | | | | 5.03 | 5.74 | 4.99 | 0.86 | 13.30 | 2.89 | | |
| Ca-amphibole | | | | | | | | | | | 0.18 |
| Orthopyroxene | | | | | | | | | | | 26.11 |
| Olivine | | | | | | | | | | | 64.52 |
| **Density** | **3.2257** | **3.0565** | **3.0552** | **3.1374** | **3.1855** | **3.0634** | **3.3822** | **3.3285** | **3.0856** | **3.4680** | **3.3125** |
| Xalm | 0.6772 | 0.3958 | 0.5795 | 0.4008 | 0.4019 | 0.4146 | 0.4434 | 0.6032 | 0.5361 | 0.3573 | 0.1671 |
| Xpyrope | 0.2926 | 0.1107 | 0.1336 | 0.5643 | 0.5656 | 0.5352 | 0.5358 | 0.3329 | 0.3954 | 0.4336 | 0.7264 |
| Xgrossular | 0.0303 | 0.4935 | 0.2868 | 0.0349 | 0.0326 | 0.0502 | 0.0208 | 0.0639 | 0.0686 | 0.2091 | 0.1065 |
| Xjad | 0.8915 | 0.3738 | 0.6565 | 0.9277 | 0.9322 | 0.8999 | 0.9575 | 0.9305 | 0.9085 | 0.4822 | 0.1854 |
| XMAcel | 0.3112 | 0.1933 | 0.1494 | 0.2726 | 0.2726 | 0.2649 | 0.2586 | 0.1841 | 0.2128 | 0.2648 | |
| XFAcel | 0.4064 | 0.2222 | 0.2647 | 0.1144 | 0.1148 | 0.1187 | 0.1278 | 0.1825 | 0.1590 | 0.1032 | |
| Xparag | 0.0216 | 0.0089 | 0.0189 | 0.0377 | 0.0380 | 0.0361 | 0.0392 | 0.0353 | 0.0349 | 0.0191 | |

thickening is discernable by the present topography (Himalaya, Tibetan plateau). It might result from mere thrusting of one plate under the other. Seismic studies have confirmed this view [42]. This thrusting of one plate under the other in this region, however, is lasting now for about 50 Ma. At the beginning of this process

Table 4
Modal content, bulk rock density (g/cm$^3$), and compositions of garnet, clinopyroxene, and phengite at 35 kbar and 900 °C resulting from the calculation with the DEKAP code applied to the rock compositions of Table 1

| | Average pelagic clay | Average sediment | Upper continental crust | Mix 1 | Mix 2 | Mix 3 | Mix 4 | Fjortoft gneiss | Saiden-bachite | MORB | Upper mantle |
|---|---|---|---|---|---|---|---|---|---|---|---|
| Coesite | 10.76 | 30.36 | 28.10 | 26.85 | 18.73 | 36.10 | 16.85 | 25.68 | 31.91 | 8.93 | |
| Rutile | 0.65 | | 0.37 | 0.88 | 0.91 | 0.83 | 0.90 | 1.24 | 0.56 | 1.10 | 0.07 |
| Clinopyroxene | 42.34 | 25.60 | 35.71 | 12.46 | 13.09 | 16.16 | 11.62 | 2.81 | 18.23 | 40.42 | 4.76 |
| K white mica | 31.25 | 25.91 | 30.40 | 35.79 | 40.56 | 29.86 | 24.82 | 24.70 | 32.00 | 0.98 | |
| Biotite | | | | | | | | | | | 0.39 |
| Garnet | 10.02 | 6.68 | 2.88 | 15.49 | 17.21 | 9.14 | 42.37 | 29.64 | 12.75 | 41.33 | 4.08 |
| Magnetite | 1.41 | | 0.25 | 2.16 | 2.28 | 1.79 | 1.75 | 1.38 | 0.60 | | 0.30 |
| Epidote | | 9.81 | 2.30 | | | | | | | 7.23 | |
| Titanite | | 1.64 | | | | | | | | | |
| Kyanite | | | | 6.36 | 7.22 | 6.13 | 1.69 | 14.54 | 3.95 | | |
| Ca-Amphibole | | | | | | | | | | | 0.18 |
| Orthopyroxene | 3.57 | | | | | | | | | | 25.64 |
| Olivine | | | | | | | | | | | 64.59 |
| **Density** | **3.3208** | **3.1929** | **3.1793** | **3.2652** | **3.2903** | **3.2154** | **3.4754** | **3.4515** | **3.2259** | **3.5245** | **3.3303** |
| Xalm | 0.6383 | 0.2739 | 0.5304 | 0.4034 | 0.4050 | 0.4153 | 0.4443 | 0.6044 | 0.5330 | 0.3323 | 0.1612 |
| Xpyrope | 0.3360 | 0.0924 | 0.1366 | 0.5568 | 0.5581 | 0.5230 | 0.5338 | 0.3306 | 0.3876 | 0.4191 | 0.7343 |
| Xgrossular | 0.0257 | 0.6337 | 0.3330 | 0.0398 | 0.0370 | 0.0616 | 0.0219 | 0.0650 | 0.0794 | 0.2486 | 0.1046 |
| Xjad | 0.8915 | 0.4283 | 0.6891 | 0.9379 | 0.9418 | 0.9102 | 0.9638 | 0.9438 | 0.9201 | 0.5002 | 0.1967 |
| XMAcel | 0.3986 | 0.2584 | 0.1910 | 0.3223 | 0.3222 | 0.3134 | 0.3075 | 0.2202 | 0.2535 | 0.3481 | |
| XFAcel | 0.4136 | 0.2130 | 0.2842 | 0.1306 | 0.1311 | 0.1351 | 0.1452 | 0.2111 | 0.1818 | 0.1213 | |
| Xparag | 0.0064 | 0.0021 | 0.0044 | 0.0082 | 0.0082 | 0.0078 | 0.0085 | 0.0076 | 0.0075 | 0.0041 | |

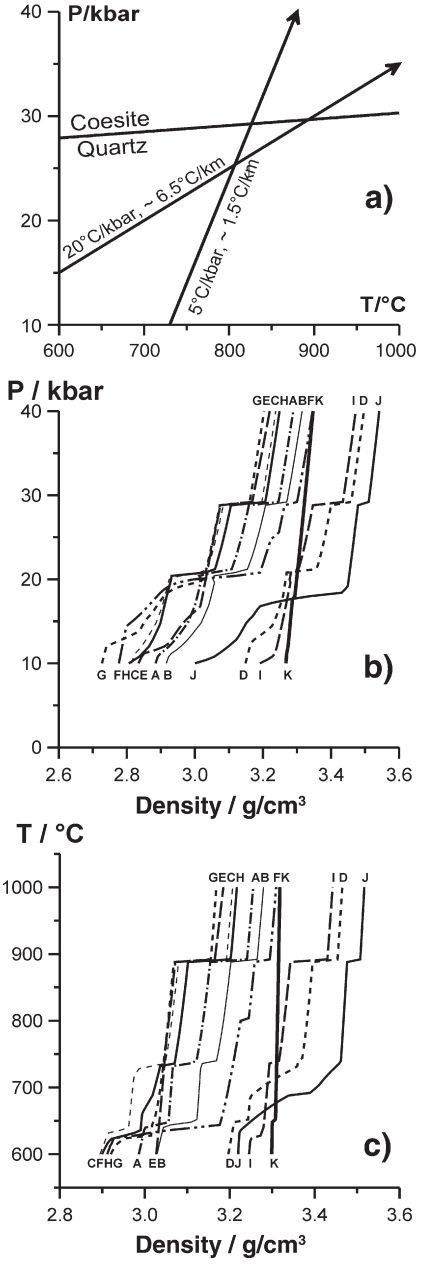


Fig. 9. Calculated density changes of the rock compositions of Table 1 (A: Mix 1, B: Mix 2, C: Mix 3, D: Mix 4, E: Average Sediment, F: Average Pelagic Clay, G: Upper Continental Crust, H: Saidenbachite, I: Fjortoft Gneiss, J: N-MORB, K: Peridotite) along *P*–*T* trajectories (a): 5 °C/kbar (b) and 20 °C/kbar (c).

ultrahigh pressure rocks formed [43] either by a slab break-off process or, more likely, in a subduction channel environment. Rocks of this environment, which had already been partially exhumed by the mass flow in the subduction channel [44], could have been extruded between the colliding plates (see [45]). The currently observed thickening, which relates to the entire lithosphere leads to a metastable state (density inversion = denser mantle above lighter mantle) and could result in delamination of this lithospheric orogenic root [46]. This process could give rise to the exhumation of crustal high pressure and ultrahigh pressure rocks as suggested by Willner et al. [47] on the basis of numerical modeling experiments, or to sinking of lower portions of the thickened continental crust together with the mantle lithosphere [45]. Thus, our calculation results might contribute to the understanding of the corresponding processes in which density contrasts play a major role. As the base of thickened orogenic crust might experience pressures close to 20 kbar (~ 70 km depth) the quartz–coesite transition cannot be invoked as in the preceding section. However, garnet and Na-rich clinopyroxene forming reactions occur in the pressure interval 10 to 20 kbar (at elevated temperatures) leading to a significant density increase of crustal rocks. According to our calculations this does not only concern metabasic rocks (eclogite formation in the pressure range 15 to 18 kbar at 600 to 800 °C) but also some metapelitic rocks (especially at pressures close to 20 kbar; see, e.g., Fig. 9). Thus, it is possible that the lower portion of the continental crust can sink into the mantle after clinopyroxene and garnet forming reactions have run over a long time interval necessary to lead to extended orogenic belts with thickened continental crust.

Based on the analysis of the timing of the Late Palaeozoic Variscan events in Western and Central Europe resulting from the collision of Gondwana and Laurussia, Massonne [45] has proposed that the sinking of continental crust into the mantle was triggered by the delamination of the lithospheric root (~ 340 Ma ago) after about 55 Ma of continuous continental thickening (beginning of the collision marked by eclogites of an exhumed subduction channel, see above). This delamination was related to extensive melt formation in the crust (abundant granitoids formed after 340 Ma) and high temperature metamorphism (see: granulite massifs in the Variscan orogenic belt). Ultrahigh pressure metamorphic rocks such as the diamondiferous quartzofeldspathic rocks (saidenbachite) of the Saxonian Erzgebirge formed contemporaneously. As this particular rock shows – even after quartz was transformed to coesite – a lower density (at 40 kbar, 800 °C: 3.257 g/cm$^3$) than that of peridotite, its return to the crust was either accomplished by separation from a large crustal fragment with bulk density higher than that of peridotite as invoked above or by partial melting of metapelites deep in the mantle. The latter reason, creating buoyancy forces, was suggested by Massonne [28] for the formation of saidenbachites. As

discussed above for the slab break-off model a concentration of upper crustal material in the continental crust (see [48] for the Bohemian Massif of the Variscan orogen) and the fertilization of the mantle at the end of an orogenic cycle [49] would also relate to the lithospheric delamination process with continental crust involved.

### 3.1.3. Sinking of fragments of ancient lower crust into the mantle — kimberlite formation

Old cratonic crust commonly shows thicknesses of 40 km or more (at the base: ≥12 kbar). Because of the geothermal gradients in such crust being significantly lower than in young orogenic crust temperatures are below 500 °C at the crustal base [50]. Such conditions are, in fact, outside our *P–T* frame but Na-rich clinopyroxene and garnet-forming reactions can be extrapolated to such low temperatures assuming relatively dry conditions. At conditions of 450 °C and 13 kbar, possible for the base of cratonic crust, such reactions, although hampered by the dry nature of lower crust [8], could have run very slowly to finally result in densities of 3.47 g/cm$^3$ for metabasic rocks (= eclogites; density of lherzolite at these conditions: 3.31 g/cm$^3$, compare with Fig. 8) or 3.23 g/cm$^3$ for a metapelitic rock of type Mix 4 (compare with Fig. 2). Thus, it is conceivable that, similar to the previously discussed crustal delamination after thickening of the continental crust, dense fragments from the base of the cratonic crust could also sink into the mantle. It is likely that such fragments, because of their chemical composition, could cause melting in deeper portions of the (hot) mantle, specific melts could find their way to the Earth's surface. Indeed, we know that kimberlites are such (relatively young) melts that exclusively occur in old cratons. In addition, the corresponding melts have formed in the deep mantle, so that they often bring diamonds to the surface, and they have unusual compositions in which typical crustal elements (K, light rare earth elements) are strongly enriched. In fact, the widely accepted hypothesis that the formation of kimberlitic melts is related to eclogites residing for a very long time in the deep mantle [51] contradicts our view of the formation of these melts but there are also new results supporting our view. Liati et al. [52] reported ages of zircons from xenoliths of the deep mantle in kimberlites from southern Namibia. These zircons showed the same age clusters as the Namibian crust (Namaqua collisional event, rifting in the Damara belt, Pan–African event). Thus, it is likely that these zircons stem from a delaminated fragment of the Namibian crust. This crustal fragment could have given rise to the formation of kimberlitic melt. Also on the basis of density considerations, Anderson [53] favours delamination of portions of basic lower crust in order to explain the formation of large amounts of melts in the mantle giving rise to form large igneous provinces (LIPs). Indeed, the discussion of crustal contamination of the corresponding basic melts is ongoing for at least two decades since Nd and Sr isotope signatures of these melts were found to be indicative for this process (e.g. $^{87}Sr/^{86}Sr > 0.706$ for Snake River Plain province, western U.S. [54] or Parana province, Brazil [55]). However, this contamination was assumed to be rather the result of assimilation of continental crust during ascent of the basic melts to the Earth's surface. In contrast, kimberlitic melts rise up so quickly that this kind of contamination can be excluded. Nevertheless, kimberlitic melts (at least so-called type II kimberlites) can also show $^{87}Sr/^{86}Sr$ ratios above 0.708 [56]. Thus, the origin of LIP magmas can, indeed, be caused by delamination of lower continental crust, however, as we think, not exclusively by basic material [53] but with additional involvement of pelitic (or even minor granitic) material. At least, evidence for crustal material triggering the generation of basic melts in the mantle comes from crustal zircons found even in unexpected environments such as the mid-oceanic ridges [57] and oceanic islands [58].

## 4. Conclusions

As outlined above major geodynamic changes of the Earth are due to density contrasts of different material in the ultrabasic mantle, basic oceanic crust, basic to intermediate lower crust, and acidic upper crust. Currently, it is the common view that only oceanic crust after transformation to eclogite can be recycled into the mantle by subduction along convergent plate boundaries due to the high density of eclogite. Our calculations have shown that other rock types such as specific metapelites could have this potential as well due to densities exceeding that of lherzolite. These high densities can, however, be attained only at relatively high pressures so that specific geodynamic environments are required for rocks of continental affinity to sink into the mantle. Three possible environments have been discussed above, 1) subduction of continental crust, 2) delamination of the continental crust after crustal thickening due to continent–continent collision, and 3) delamination of continental crust at the base of thick cratonic crust. All these three environments bear the potential of recycling continental material into the mantle. Furthermore it is of importance to note that these environments could have formed only relatively late (~1 Ga ago) in the history of the Earth. At least for processes 2) and 3) crustal thickening and/or low geothermal gradients are required to overstep mineral

reactions causing high densities especially of basic and pelitic material of the continental crust.

## Acknowledgments

This work was supported by a stipend of the Alexander-von-Humboldt Foundation (to TVG). Helpful comments by an anonymous reviewer are highly appreciated.

## References

[1] W.G. Ernst, S.M. Peacock, A thermotectonic model for preservation of ultrahigh-pressure phases in metamorphosed continental crust, in: G.E. Behout, D.W. Scholl, S.H. Kirby, J. Platt (Eds.), Subduction — Top to Bottom, Am. Geophys. Union, Geophys. Monograph, vol. 96, 1996, pp. 171–178.

[2] P. Matte, Continental subduction and exhumation of HP rocks in Paleozoic orogenic belts: uralides and variscides, Geol. Fören. Stockh. Förh. 120 (1998) 209–222.

[3] P.J. O'Brien, The fundamental Variscan problem: high-temperature metamorphism at different depths and high-pressure metamorphism at different temperatures, in: W. Franke, V. Haak, O. Oncken, D. Tanner (Eds.), Orogenic Processes: Quantification and Modelling in the Variscan Belt, Geol. Soc. London Spec. Publ., vol. 179, 2000, pp. 369–386.

[4] C. Chopin, Coesite and pure pyrope in high grade blueschists of the Western Alps: a first record and some consequences, Contrib. Mineral. Petrol. 86 (1984) 107–118.

[5] N.V. Sobolev, V.S. Shatsky, Diamond inclusions in garnets from metamorphic rocks: an environment for diamond formation, Nature 343 (1990) 742–745.

[6] H.-J. Massonne, A new occurrence of microdiamonds in quartzofeldspathic rocks of the Saxonian Erzgebirge, Germany, and their metamorphic evolution, Proc. 7th Int. Kimberlite Conf., 1999, pp. 533–539.

[7] R. Bousquet, B. Goffé, P. Henry, X. Le Pichon, C. Chopin, Kinematic, thermal and petrological model of the Central Alps: Lepontine metamorphism in the upper crust and eclogitisation of the lower crust, Tectonophysics 273 (1997) 105–127.

[8] M.L. Leech, Arrested orogenic development: eclogitization, delamination, and tectonic collapse, Earth Planet. Sci. Lett. 185 (2001) 149–159.

[9] T.J.B. Holland, R. Powell, An internally consistent thermodynamic data set for phases of petrological interest, J. Metamorph. Geol. 16 (1998) 309–343.

[10] J. Dale, T.J.B. Holland, R. Powell, Hornblende–garnet–plagioclase thermobarometry: a natural assemblage calibration of the thermodynamics of hornblende, Contrib. Mineral. Petrol. 140 (2000) 353–362.

[11] R. Powell, T.J.B. Holland, Relating formulations of the thermodynamics of mineral solid solution: activity modeling of pyroxenes, amphiboles and micas, Am. Mineral. 84 (1999) 1–14.

[12] T.J.B. Holland, R. Powell, Mixing properties and activity–composition relationships of chlorites in the system MgO–FeO–$Al_2O_3$–$SiO_2$–$H_2O$, Eur. J. Mineral. 10 (1998) 395–406.

[13] T.J.B. Holland, S.A.T. Redfern, R. Powell, Volume behaviour of hydrous minerals at high pressure and temperature: II compressibilities of lawsonite, zoisite, clinozoisite and epidote, Am. Mineral. 81 (1996) 341–348.

[14] V.L. Vinograd, Thermodynamics of mixing and ordering in the diopside–jadeite system: I. A CVM model, Mineral. Mag. 66 (2002) 513–536.

[15] V.L. Vinograd, Thermodynamics of mixing and ordering in the diopside–jadeite system: II. A polynomial fit to the CVM results, Mineral. Mag. 66 (2002) 537–545.

[16] T. Will, M. Okrusch, E. Schmädicke, G. Chen, Phase relations in the greenschist–blueschist–amphibolite–eclogite facies in the system $Na_2O$–CaO–FeO–MgO–$Al_2O_3$–$SiO_2$–$H_2O$ (NCFMASH), with application to metamorphic rocks from Samos, Greece, Contrib. Mineral. Petrol. 132 (1998) 85–102.

[17] T.V. Gerya, W.V. Maresch, A.P. Willner, D.D. van Reenen, C.A. Smit, Inherent gravitational instability of thickened continental crust with regionally developed low- to medium-pressure granulite facies metamorphism, Earth Planet. Sci. Lett. 190 (2001) 221–235.

[18] D.K. Tinkham, C.A. Zuluaga, H.H. Stowell, Metapelite phase equilibria modeling in MnNCKFMASH: the effect of variable $Al_2O_3$ and MgO/(MgO+FeO) on mineral stability, Geol. Mater. Res. 3 (2001) 1–42.

[19] R. Coggan, T.J.B. Holland, Mixing properties of phengitic micas and revised garnet–phengite thermometers, J. Metamorph. Geol. 20 (2002) 683–696.

[20] C.J. Wei, R. Powell, L.F. Zhang, Eclogites from the south Tianshan, NW China: petrological characteristic and calculated mineral equilibria in the $Na_2O$–CaO–FeO–MgO–$Al_2O_3$–$SiO_2$–$H_2O$ system, J. Metamorph. Geol. 21 (2003) 163–179.

[21] H.-J. Massonne, W. Schreyer, Stability field of the high- pressure assemblage talc+phengite and two new phengite barometers, Eur. J. Mineral. 1 (1989) 391–410.

[22] C. Wei, R. Powell, Calculated phase relations in high-pressure metapelites in the system NKFMASH ($Na_2O$–$K_2O$–FeO–MgO–$Al_2O_3$–$SiO_2$–$H_2O$), J. Petrol. 45 (2004) 183–202.

[23] E.M. Mahar, J.M. Baker, R. Powell, T.J.B. Holland, N. Howell, The effect of Mn on mineral stability in metapelites, J. Metamorph. Geol. 15 (1997) 223–238.

[24] N. Le Breton, A.B. Thompson, Fluid-absent (dehydration) melting of biotite in metapelites in the early stages of crustal anatexis, Contrib. Mineral. Petrol. 99 (1988) 226–237.

[25] D. Vielzeuf, J.R. Holloway, Experimental determination of the fluid-absent melting relations in the pelitic system: consequences for crustal differentiation, Contrib. Mineral. Petrol. 98 (1988) 257–276.

[26] A.E. Patiño Douce, T.C. McCarthy, Melting of crustal rocks during continental collision and subduction, in: B.R. Hacker, J.G. Liou (Eds.), When Continents Collide: Geodynamics and Geochemistry of Ultrahigh-Pressure Rocks, Kluwer Acad. Publ., 1998, pp. 27–55.

[27] L.F. Dobrzhinetskaya, E.A. Eide, R.B. Larsen, B.A. Sturt, R.G. Trønnes, D.C. Smith, W.R. Taylor, T.V. Posukhova, Diamond in metamorphic rocks of the Western Gneiss Region in Norway, Geology 23 (1995) 597–600.

[28] H.-J. Massonne, A comparison of the evolution of diamondiferous quartz-rich rocks from the Saxonian Erzgebirge and the Kokchetav Massif: are so-called diamondiferous gneisses magmatic rocks? Earth Planet. Sci. Lett. 216 (2003) 345–362.

[29] S.M. McLennan, Sediments and soils: chemistry and abundances, in: T.J. Ahrens (Ed.), Rock Physics and Phase Relations, A Handbook of Physical Constants, AGU Reference Shelf, vol. 3, 1995, pp. 8–19.

[30] S. Maaløe, K. Aoki, The major element composition of the upper mantle estimated from the composition of lherzolites, Contrib. Mineral. Petrol. 63 (1977) 161–173.

[31] J.-G. Schilling, M. Zajac, R. Evans, T. Johnston, W. White, J.D. Devine, R. Kingsley, Petrological and geochemical variations along the Mid-Atlantic Ridge from 27°N to 73°N, Am. J. Sci. 283 (1983) 510–586.
[32] T.V. Gerya, D.A. Yuen, Rayleigh–Taylor instabilities from hydration and melting propel "cold plumes" at subduction zones, Earth Planet. Sci. Lett. 212 (2003) 47–62.
[33] T.V. Gerya, D.A. Yuen, E.O.D. Sevre, Dynamical causes for incipient magma chambers above slabs, Geology 32 (2004) 89–92.
[34] T.V. Gerya, B. Stöckhert, 2-D numerical modeling of tectonic and metamorphic histories at active continental margins, Int. J. Earth Sci. 95 (2006) 250–274.
[35] J.G. Liou, S. Maruyama, W.G. Ernst, Seeing a mountain in a grain of garnet, Science 276 (1997) 48–49.
[36] J.H. Davies, F. von Blanckenburg, Slab breakoff: a model of lithospheric detachment and its test in the magmatism and deformation of collisional orogens, Earth Planet. Sci. Lett. 129 (1995) 85–102.
[37] M.J. Kohn, C.D. Parkinson, Petrologic case for Eocene slab breakoff during the Indo–Asian collision, Geology 30 (2002) 591–595.
[38] F.-L. Liu, Z.-Q. Xu, I. Katayama, J.-S. Yang, S. Maruyama, J.G. Liou, Mineral inclusions in zircons of para- and orthogneiss from pre-pilot drillhole CCSD-PP1, Chinese Continental Scientific Drilling Project, Lithos 59 (2001) 199–215.
[39] J. Liu, K. Ye, S. Maruyama, B. Cong, H. Fan, Mineral inclusions in zircon from gneisses in the ultrahigh-pressure zone of the Dabie Mountains, China, J. Geol. 109 (2001) 523–535.
[40] X. Liu, B.-m. Jahn, S. Dong, H. Li, R. Oberhänsli, Neoproterozoic granitoid did not record ultrahigh-pressure metamorphism from the southern Dabieshan of China, J. Geol. 111 (2003) 719–732.
[41] T. Hirajima, D. Nakamura, The Dabie Shan–Sulu orogen, in: D.A. Carswell, R. Compagnoni (Eds.), Ultrahigh Pressure Metamorphism, EMU Notes Mineral, vol. 5, 2003, pp. 105–144.
[42] H.-W. Zhou, M.A. Murphy, Tomographic evidence for wholesale underthrusting of India beneath the entire Tibetan plateau, J. Asian Earth Sci. 25 (2005) 445–457.
[43] H.-J. Massonne, P.J. O'Brien, The Bohemian Massif and the NW Himalaya, in: D.A. Carswell, R. Compagnoni (Eds.), Ultrahigh Pressure Metamorphism, EMU Notes Mineral, vol. 5, 2003, pp. 145–187.
[44] B. Stöckhert, T.V. Gerya, Pre-collisional high pressure metamorphism and nappe tectonics at active continental margins: a numerical simulation, Terra Nova 17 (2005) 102–110.
[45] H.-J. Massonne, Involvement of crustal material in delamination of the lithosphere after continent–continent collision, Int. Geol. Rev. 47 (2005) 792–804.
[46] B. Schott, H. Schmeling, Delamination and detachment of a lithospheric root, Tectonophysics 296 (1998) 225–247.
[47] A.P. Willner, E. Sebazungu, T.V. Gerya, W.V. Maresch, A. Krohe, Numerical modelling of PT-paths related to rapid exhumation of high-pressure rocks from the crustal root in the Variscan Erzgebirge Dome (Saxony/Germany), J. Geodyn. 33 (2002) 281–314.
[48] A. Wittenberg, C. Vellmer, H. Kern, K. Mengel, The Variscan lower continental crust: evidence for crustal delamination from geochemical and petrophysical investigations, in: W. Franke, V. Haak, O. Oncken, D. Tanner (Eds.), Orogenic Processes: Quantification and Modelling in the Variscan Belt, Geol. Soc. London Spec. Publ., 179, 2000, pp. 401–414.
[49] T. Wenzel, D.F. Mertz, R. Oberhänsli, T. Becker, P.R. Renne, Age, geodynamic setting and mantle enrichment processes of a K-rich intrusion from the Meissen massif (northern Bohemian massif) and implications for related occurrences from the mid-European Hercynian, Geol. Rundsch. 86 (1997) 556–570.
[50] K.C. Condie, Plate Tectonics and Crustal Evolution, 3rd ed., Pergamon Press, Oxford, 1989, 476 p.
[51] C.R. Neal, L.A. Taylor, J.P. Davidson, P. Holden, A.N. Halliday, P.H. Nixon, J.B. Paces, R.N. Clayton, T.K. Mayeda, Eclogites with oceanic crustal and mantle signatures from the Bellsbank kimberlite, South Africa, part 2: Sr, Nd and O isotope geochemistry, Earth Planet. Sci. Lett. 99 (1990) 362–379.
[52] A. Liati, L. Franz, D. Gebauer, C. Fanning, The timing of mantle and crustal events in South Namibia, as defined by SHRIMP-dating of zircon domains from a garnet peridotite xenolith of the Gibeon Kimberlite Province, J. Afr. Earth Sci. 39 (2004) 147–157.
[53] D.L. Anderson, Large igneous provinces, delamination, and fertile mantle, Elements 1 (2005) 271–275.
[54] M.A. Menzies, W.P. Leeman, C.J. Hawkesworth, Geochemical and isotopic evidence for the origin of continental flood basalts with particular reference to the Snake River Plain, Idaho, U.S.A. Philos. Trans. R. Soc. Lond., A 310 (1984) 643–660.
[55] C.J. Hawkesworth, M.S.M. Mantovani, P.N. Taylor, Z. Palacz, Evidence from the Paraná of south Brazil for a continental contribution to Dupal basalts, Nature 322 (1986) 356–359.
[56] C.B. Smith, J.J. Gurney, E.M.W. Skinner, C.R. Clement, N. Ebrahim, Geochemical character of southern Africa kimberlites: a new approach based on isotopic constraints, Trans. Geol. Soc. S. Afr. 88 (1985) 267–280.
[57] J. Pilot, C.-D. Werner, F. Haubrich, N. Baumann, Paleozoic and Proterozoic zircons from the Mid-Atlantic ridge, Nature 393 (1998) 676–679.
[58] U. Schaltegger, H. Amundsen, B. Jamtveit, M. Frank, W.L. Griffin, K. Grönvold, R. Tronnes, T. Torsvik, Contamination of OIB by underlying ancient continental lithosphere: U–Pb and Hf isotopes in zircons question EM1 and EM2 mantle components, Geochim. Cosmochim. Acta, Suppl. 1 (2002) A673.